Hindawi
Shock and Vibration
Volume 2018, Article ID 3616942, 9 pages
https://doi.org/10.1155/2018/3616942

Research Article

Experimental Study on the Stress Sensitivity and Influence Factors of Shale under Varying Stress

Zhonghu Wu,[1] Yujun Zuo,[2] Shanyong Wang,[3] Jibin Sunwen,[2] and Leilei Liu[4]

[1]*College of Civil Engineering, Guizhou University, Guiyang 550025, China*
[2]*Mining College, Guizhou University, Guiyang 550025, China*
[3]*ARC Centre of Excellence for Geotechnical Science and Engineering, The University of Newcastle, Australia, University Drive, Callaghan, NSW 2308, Australia*
[4]*Department of Civil and Environmental Engineering, The Hong Kong Polytechnic University, Kowloon, Hong Kong*

Correspondence should be addressed to Yujun Zuo; zuo_yujun@163.com and Leilei Liu; leilei.liu@connect.polyu.hk

Received 3 October 2017; Revised 29 December 2017; Accepted 6 May 2018; Published 11 July 2018

Academic Editor: Caiping Lu

Shale reservoirs are characterized by extremely low permeability and high clay content. To further study the stress sensitivity of a shale reservoir, the Lower Cambrian shale in north Guizhou was utilized. Through laboratory testing, the relationships between the shale porosity and permeability and the effective stress were established, and the stress sensitivity of shale was analysed. The mechanical properties and mineral composition of this shale were studied by rock mechanics testing and X-ray diffraction. The main factors affecting the stress sensitivity were analysed. The results show that the porosity and permeability of this shale decrease with increasing effective stress; the shale reservoir permeability damage rate is 61.44 ~ 73.93%, with an average of 69.92%; the permeability stress sensitivity coefficient is 0.04867 ~ 0.05485 MPa^{-1}, with an average of 0.05312 MPa^{-1}; and the shale reservoir stress sensitivity is strong. Shale stress sensitivity is related to the rock mineral composition and rock mechanical properties. The higher the clay content in the mineral composition, the lower the elastic modulus of shale, the higher the compressibility, and the greater the stress sensitivity coefficient.

1. Introduction

Shale gas is an important unconventional natural gas whose higher content, long production cycle, and other advantages have earned it extensive attention across the world. It is one of the most realistic alternatives to conventional oil and gas resources, giving it an important strategic position [1–10]. Porosity and permeability are important reservoir characteristics that directly affect shale gas production. The pore characteristics influence the storage capacity, occurrence state, and migration capacity of shale gas within the reservoir. Permeability is a measure of the ability of porous media to allow fluid flow and is the key parameter of shale gas production capacity [11, 12]. Experimental research has been an important means to study the permeability of shale gas; some scholars have analysed the permeability characteristics of shale gas accounting for Klinkenberg's effect and the shale gas migration form [13–18]. Nelson [19] found the nano pores in the shale, which revealed a huge shale gas storage sites, and increased the study of the spatial scale of shale gas seepage.

Many scholars have studied the relationship between the permeability and stress of conventional oil and gas reservoirs and have achieved remarkable results [20–24]. The definitions of the volume compression coefficient and pore compression coefficient of rock and their relations have been given explicitly, the concept of the pore compression coefficient and stress sensitivity coefficient have been introduced into reservoir engineering problems, and the effect of the deformation of the pore volume change and permeability has been analysed [24, 25]. Compared with conventional oil and gas reservoirs, shale gas formations and reservoirs have the same layer and geological characteristics, including obvious elastic and plastic deformation and stress sensitivity. Scholars have extensively studied the stress sensitivity of

Table 1: Basic data of shale samples.

Sample ID	Test core size		Moisture	Permeability/$10^{-3}\mu m^2$	Porosity/%
	Diameter, mm	Length, mm			
1	25.23	50	Dry	0.0060	1.67
2	25.27	51	Dry	0.0052	1.62
3	25.21	50.5	Dry	0.0071	1.85
4	25.30	51	Dry	0.0073	1.80
5	25.20	49	Dry	0.0056	1.56

shale matrix. Dong et al. [26] studied the porosity and permeability of shale samples, and the testing results showed that the stress sensitivity of shale was stronger than that of sandstone, and the change of porosity and permeability meets the power relationship under effective stress. Chalmers [27] used the pulse method to show that shale has strong stress sensitivity by changing the effective stress. Kwon et al. [28] researched the influence of internal and external pressure changes on shale stress sensitivity by the pulse method. Reyes and Osisanya [29] measured 4 shale cores from the Oklahoma area using the steady state method, and the results showed that the stress sensitivity of shale exhibited the highest degree of exponential fitting. Although various studies have investigated the stress sensitivity of shale, the previous studies were mostly intuitive analyses of the experimental results, rock mineral composition, and rock mechanical properties; several factors have rarely been analysed.

This study utilizes the overburden pressure permeability and porosity measurement experiment of the Lower Cambrian shale core to evaluate the shale stress sensitivity. At the same time, for a shale reservoir with a series of characteristics different from conventional reservoirs, our study combined X-ray diffraction and rock mechanics testing to analyse the factors affecting the shale stress sensitivity. It is anticipated that our study will have theoretical and practical significance to revealing the law of permeability stress sensitivity of shale reservoirs and to the rational and effective exploitation of shale gas resources.

2. Experimental Method

2.1. Experimental Conditions for Permeability of Shale under Overburden Pressure. The experimental samples were from the Lower Cambrian Niutitang Formation in north Guizhou, with shale composed mainly of siliceous shale and grey-to-black shale with high TOC content ranging from 3.54 wt% to 8.12 wt%, with an average TOC content of 7.24 wt%. The brittleness index is in the range of 19.14-51.87. The sample diameter is approximately 25 mm, the length is approximately 50 mm, and the sample basic data are shown in Table 1.

Using an FYKS-2 high-temperature coating porosity and permeability measuring instrument, the name of the manufacturer is Jiangsu Haian Petroleum Instrument Factory in China. The test was conducted at a temperature of 150 C°; the porosity and permeability were measured by using nitrogen gas. All data acquisition and recordings were calculated through the computer. To study the influence of stress on the porosity and permeability of shale, the change of effective stress was simulated by increasing the effective confining pressure of shale. The porosity and permeability under effective confining pressure were measured, and the relationships of the shale reservoir porosity and permeability with stress were analysed. Each confining pressure (3, 5, 7, 9, and 11 MPa) and each stress point were sustained for a sufficiently long time (to maintain balance of at least 30 min), and the gas permeability at each stress was determined.

3. Results and Discussion

3.1. The Relationships of Porosity and Permeability with Stress for Shale. The relationships of the porosity and permeability with the effective stress are shown in Figure 1.

3.1.1. Relationship between Shale Porosity and Effective Stress. As seen in Figure 1, the relationship between the porosity of shale samples and the effective stress follows a negative exponential function. The porosity of the shale reservoir decreases with increasing effective stress as a negative exponential function. Through the regression analysis of the experimental results, the relationship can be defined as follows:

$$\varphi = \varphi_0 e^{-mp} \quad (1)$$

where φ is the porosity under a specific effective stress, φ_0 is the porosity under the initial effective stress, m is the coefficient of compressibility (MPa^{-1}), and p is the effective stress (MPa).

The experimental results of 5 samples under varying effective confining pressure are shown in Table 2. In Table 2, the compression coefficient of the Lower Cambrian shale is from 0.1093 to 0.2814 MPa^{-1}, with an average of 0.1734 MPa^{-1}.

3.1.2. Relationship between Gas Permeability and Effective Stress of Shale. As seen in Figure 1, the gas permeability and effective stress of shale samples are also subject to a negative exponential function. The permeability of the shale reservoir decreases with increasing effective stress in the negative exponential function; the relationship can be shown as

$$K = K_0 e^{-np} \quad (2)$$

where K is the permeability under a specific effective stress ($10^{-3}\mu m^2$), K_0 is the permeability under the initial effective

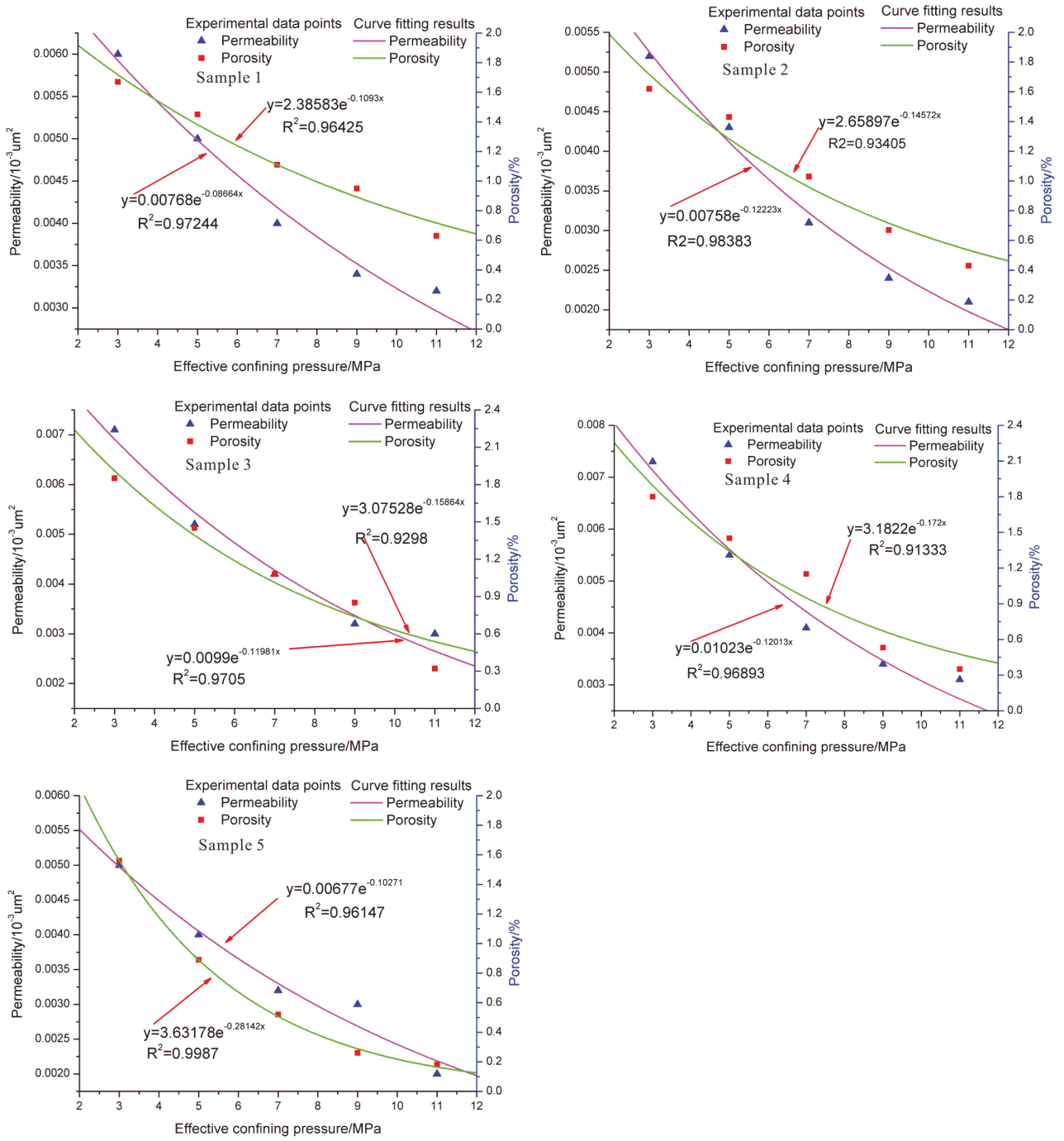

FIGURE 1: Relationships of the permeability and porosity with the effective confining pressure of shale.

stress ($10^{-3}\mu m^2$), and n is the stress sensitivity coefficient of permeability (MPa^{-1}).

The experimental results of 5 samples under the overburden pressure are shown in Table 2.

In Table 2, the stress sensitivity coefficient of the shale reservoir is 0.08664 to 0.12223 MPa $^{-1}$, with an average of 0.11030 MPa $^{-1}$.

3.2. Stress Sensitivity Analysis of Shale Reservoirs. At present, there is no industry standard for shale stress sensitivity. Our experiment referenced the petroleum and natural gas industry standards of China (SY/T 5336, 5358, 6385). The change of effective stress was simulated by increasing the effective confining pressure of shale, and the change of the permeability of shale samples with changing effective confining

Table 2: Statistic analysis results of the relationships of the porosity and permeability of shale with the effective stress.

Sample ID	Compressibility m/MPa^{-1}	Porosity φ_0/%	R_1^2	Coefficient n/MPa^{-1}	Permeability $K_0/10^{-3}\mu m^2$	R_2^2
1	0.1093	2.3858	0.9643	0.08664	0.00768	0.9724
2	0.1457	2.6589	0.9341	0.12223	0.00758	0.9838
3	0.1586	3.0753	0.9298	0.11981	0.00990	0.9705
4	0.1720	3.1822	0.9133	0.12013	0.01023	0.9689
5	0.2814	3.6318	0.9987	0.10271	0.00671	0.9615
Maximum value	0.2814	3.6318	0.9987	0.12223	0.01023	0.9838
Minimum value	0.1093	2.3858	0.9133	0.08664	0.00671	0.9615
Average value	0.1734	2.9868	0.9480	0.11030	0.00842	0.9714

R_1^2 is the correlation coefficient of the porosity and effective stress of shale; R_2^2 is the correlation coefficient of the permeability and effective stress of shale.

pressure was measured. The degree of stress sensitivity of the shale reservoir was then analysed.

3.2.1. Shale Reservoir Stress Sensitivity Parameter. According to the petroleum and natural gas industry standards of China (SY/T 5336), the authors used the permeability damage rate and the stress sensitivity coefficient to evaluate the sensitivity.

(1) Permeability Damage Rate. The permeability damage rate is reflected in the percentage of the permeability damage of the shale reservoir under the effective stress. The permeability damage rate D_{K2} caused by the stress sensitivity can be calculated according to

$$D_k = \frac{K_1 - K_{\min}}{K_1} \times 100\% \quad (3)$$

where D_k is the maximum value of permeability damage caused by the process of increasing stress to the highest point; K_1 is the permeability at a given effective pressure p; and $K_{\min}$ is the minimum permeability obtained at the highest effective confining pressure achieved in this study.

(2) Stress-Sensitive Coefficient, the Definition of the Shale Stress Sensitivity Coefficient [30].

$$\alpha_K = -\frac{1}{K_0}\frac{\partial K}{\partial p} \quad (4)$$

Equation (4) reveals that the larger the value of α_K is, the more sensitive the permeability of shale samples to the change of effective pressure. Under the same change of effective pressure, the permeability of the shale is larger for a larger α_K. Conversely, the smaller the value of α_K is, the less sensitive the shale sample permeability is.

3.2.2. Relationship between Stress Sensitivity Parameters and Effective Stress of Shale. Five shale samples were tested. When the effective pressure increased to 11 MPa, the shale permeability was $0.00198\times10^{-3}\mu m^2$ to $0.00296\times10^{-3}\mu m^2$, and the average was $0.00249\times10^{-3}\mu m^2$. The permeability damage rate was 61.44 ~ 73.93%, with an average of 69.92%. According to the petroleum and natural gas industry standard (SY/T 5336, 5358, 6385), it is known that the permeability damage degree of this area is moderately strong. The permeability stress sensitivity coefficient was 0.04867~0.05485 MPa^{-1}, with an average of 0.05312 MPa^{-1}. Therefore, the stress sensitivity of shale reservoirs in this area is strong. The minimum average stress sensitivity coefficient of sample No. 1 of the five samples was $0.04867\times10^{-3}\mu m^2$. The maximum average stress sensitivity coefficient of sample 2 was $0.05511\times10^{-3}\mu m^2$. The stress sensitivity evaluation parameters of the 5 shale samples tested are shown in Table 3.

Figure 2 shows the evolution of the permeability damage rate and the stress sensitivity coefficient under varying effective pressure for the 5 samples. The stress sensitivity coefficient of the shale reservoir decreases with increasing effective stress, and the permeability damage rate increases with increasing effective stress (Figure 2).

The stress sensitivity coefficient of the shale reservoir changes similarly in pressure ranges 0-11 MPa for the 5 shale samples. The stress sensitivity coefficient of the shale reservoir decreases with increasing effective stress. At the same time, the damage rate of permeability increases with increasing effective stress.

3.3. Discussion and Analysis of Shale Stress Sensitivity Factor

3.3.1. Component Analysis of Shale Mineral. There is a difference in the degree of deformation of different rock minerals under compression, which is mainly related to the skeleton structure and mineral composition of the rock. The mineral composition of the 5 samples was analysed by X-ray diffraction, and the test results are shown in Figure 3.

As seen in Figure 3, shale samples consist mainly of quartz, plagioclase, K-feldspar, pyrite, clay minerals, calcite, and dolomite, and the quartz content is greater than 50%. The stress sensitivity of sample 2 is the highest; its clay content is the highest, reaching 30%, and the quartz content is 50%. The stress sensitivity of sample No. 1 is the weakest; its quartz content is the highest, more than 80%, and the clay content is 3%. Samples No. 3 and No. 4 have similar contents of quartz and clay minerals, and the stress sensitivity coefficients are also similar. This shows that quartz and clay mineral are the two mineral components that most significantly control the

Table 3: Evaluation parameters of stress sensitivity for the shale reservoir.

Sample ID	Permeability/10^{-3} μm^2		Permeability damage rate/%	Average value of stress sensitivity coefficient/MPa^{-1}
	3 MPa	11 MPa		
1	0.00592	0.00296	61.44	0.04867
2	0.00525	0.00198	73.93	0.05511
3	0.00691	0.00265	73.23	0.05481
4	0.00713	0.00273	73.32	0.05485
5	0.00493	0.00218	67.69	0.05218
Maximum value	0.00713	0.00296	73.93	0.05485
Minimum value	0.00493	0.00198	61.44	0.04867
Average value	0.00603	0.00249	69.92	0.05312

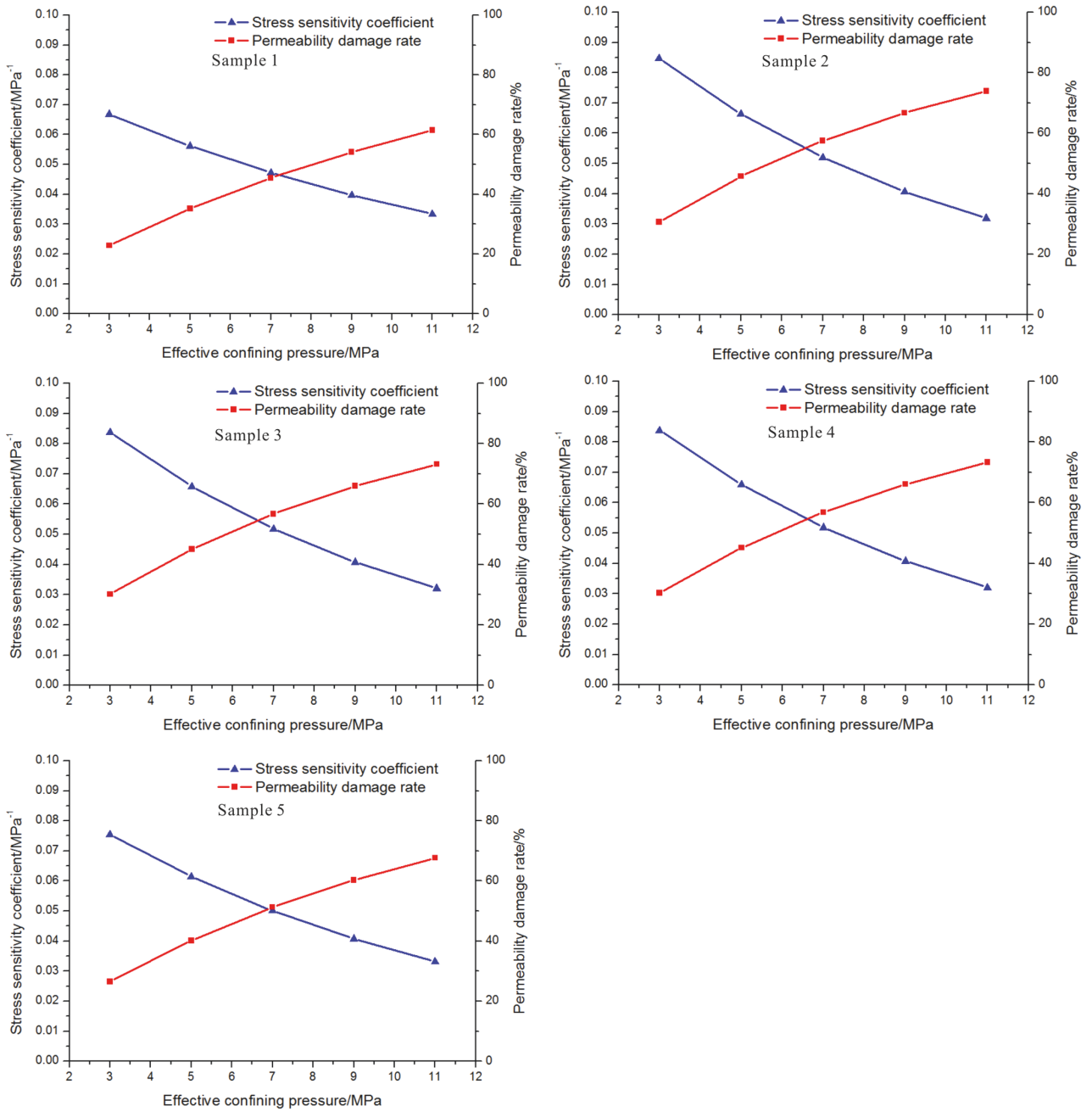

Figure 2: Relationships of the permeability damage rates and stress sensitivity coefficient with the effective stress.

Table 4: Shale elastic modulus and Poisson's ratio.

Sample ID	Elastic modulus (GPa)	Poisson's ratio
1	27.53	0.24
2	20.46	0.26
3	24.15	0.22
4	23.82	0.27
5	25.37	0.29

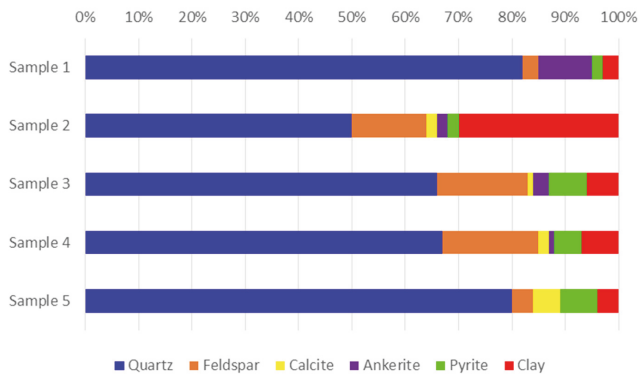

Figure 3: Mineral composition of the Lower Cambrian Niutitang Formation shale.

shale compressibility. In general, rocks with high argillaceous content are more prone to deformation than those with low argillaceous content. At the same time, porosity decreases with increasing effective stress, but the decreasing trends are not the same, which is mainly related to the distribution of the shale microstructure and mineralogical composition. Overall, the lower the quartz content and the higher the clay content are, the stronger the stress sensitivity of shale is.

3.3.2. Rock Mechanics Analysis of Shale. Shale mechanical parameters not only provide the necessary technical basis for the design of horizontal drilling and fracturing parameters in the exploitation of hydraulic fracturing but also are an important factor affecting the shale stress sensitivity. Therefore, uniaxial compression tests were used to test the mechanical parameters of 5 shale samples to further study the relationship between the mechanical properties and stress sensitivity. Young's modulus and Poisson's ratio for the 5 samples according to the experimental results are shown in Table 4 and Figure 4.

The elastic modulus of rock is an important parameter to determine the compressibility of reservoir rock, and the compression coefficient of rock is related to the volumetric modulus of the skeleton: the harder the skeleton is, the smaller the compression coefficient is [31]. The compression coefficient of rock is also related to the porosity of the rock: the greater the porosity is, the higher the compression coefficient is. The relationship of the compression coefficient of rock, the porosity, and the skeleton compression coefficient is

$$C_p = \frac{\varphi}{1-\varphi} C_s \tag{5}$$

where C_s is the skeleton compression coefficient of rock; C_p is the coefficient of rock compressibility; and φ is rock porosity.

Elgmati [32] gave the constitutive model of the volumetric strain as a function of Young's modulus and Poisson's ratio; the expression of volumetric strain in the elastic deformation of rock is derived by the constitutive model

$$\varepsilon_v = C_s \frac{(1+\nu)\left(\varepsilon_x + \varepsilon_y + \varepsilon_z\right)}{3\left[\nu\varepsilon_x + \nu\varepsilon_y + (1-\nu)\,\varepsilon_z\right]} \left(\sigma_t - p\right) \tag{6}$$

where ε_v is the volumetric strain; $\varepsilon_x, \varepsilon_y, \varepsilon_z$ are x, y, z in the direction of the strain; ν is Poisson's ratio; and σ_t is the overburden stress.

According to (6), the volumetric strain is proportional to the coefficient of skeleton compression. The skeleton compression coefficient of the rock can be expressed as

$$C_s = \frac{3\,(1-2\nu)}{E} \tag{7}$$

Formula (7) shows that the greater the Young modulus of the rock is, the smaller the volume strain is and the less deformed the rock is. The relationship between Young's modulus and the stress sensitivity index of 5 samples is shown in Figure 5. The experimental results are consistent with the theoretical analysis of the elastic modulus and the stress sensitivity.

4. Conclusions

(1) The experimental results show that the effective stress and the permeability and porosity of the Lower Cambrian shale in north Guizhou Province follow a negative exponential function, and the correlation coefficient is greater than 0.9. Under compressive stress, shale reservoirs have normal compressive deformation with increasing stress, while the porosity and permeability of the shale reservoir decrease.

(2) The compression coefficient m of the Lower Cambrian shale reservoir is 0.1093 ~ 0.2814 MPa^{-1}, and the average is 0.1734 MPa^{-1}; the regression coefficient of stress sensitivity is 0.08664 ~ 0.12223 MPa^{-1}, and the average is 0.11030 MPa^{-1}. The compressibility and stress sensitivity regression coefficients can be used to calculate the porosity and permeability of a shale reservoir under the present formation pressure, which is very important for shale reservoir physical property research.

(3) The shale permeability damage rate was 61.44 ~ 73.93%, with an average of 69.92%. The petroleum and natural gas industry standards (SY/T 5336, 5358, 6385) show that the degree of permeability damage in the region is moderately strong. The stress sensitivity coefficient of permeability is 0.04867 ~ 0.05485 MPa^{-1}, and the average is 0.05312 MPa^{-1}, so the stress sensitivity of the shale reservoir is strong.

(4) The degree of shale stress sensitivity is related to the rock mineral composition and rock mechanics properties. The higher the clay mineral content in the mineral composition is, the smaller the elastic modulus of the shale is, the higher the compressibility is, and the greater the stress sensitivity coefficient is.

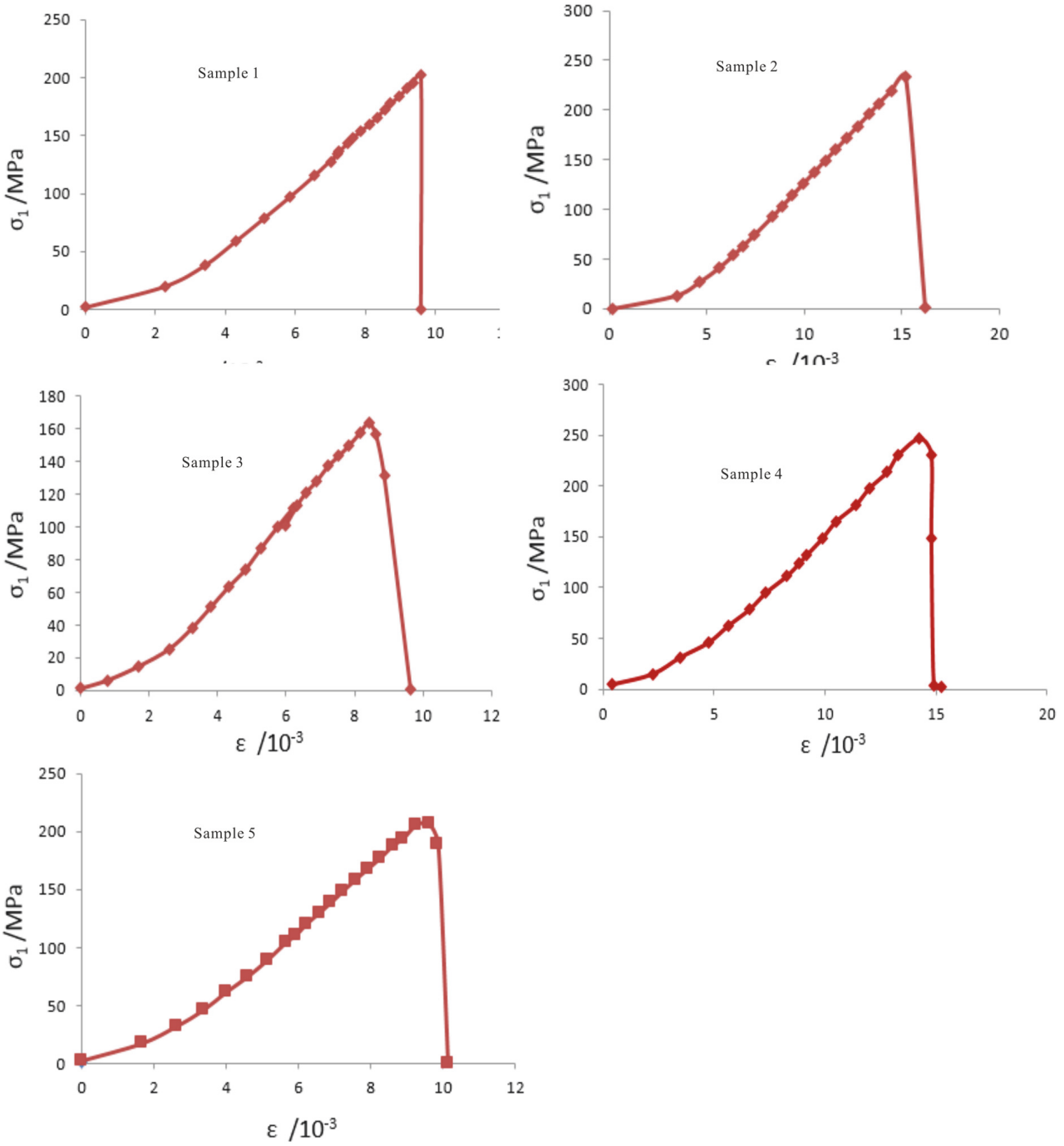

Figure 4: Stress-strain curve of samples.

Conflicts of Interest

The authors declare that there are no conflicts of interest regarding the publication of this paper.

Acknowledgments

This study was supported by the Talent introduction Project of Guizhou University (Project no. [2017]63), the Cultivation Project of Guizhou University ïijĹProject no. [2017]5788-49), the Project of Special Fund for Science and Technology of Water Resources Department of Guizhou Province (Project no. KT201804), the First-class Discipline Construction Project in Guizhou Province (Project no. QYNYL[2017]0013), the National Natural Science Foundation of China (Project nos. 51574093 and 51774101), the Major Application Foundation Research Project of Guizhou Province (Project no. JZ2014-2005), and the High-Level

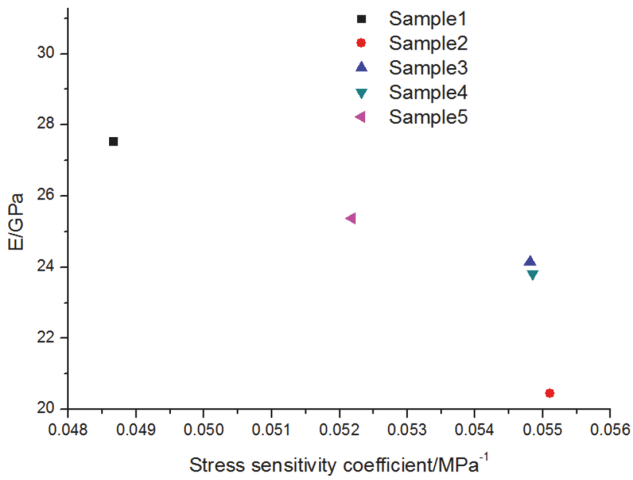

Figure 5: Elastic modulus versus stress sensitivity coefficient.

Innovative Talents Training Project in Guizhou Province (Project no. 2016-4011).

References

[1] J. F. W. Gale, S. E. Laubach, J. E. Olson, P. Eichhubl, and A. Fall, "Natural fractures in shale: A review and new observations," *AAPG Bulletin*, vol. 98, no. 11, pp. 2165–2216, 2014.

[2] H. Jiang, B. Ju, and Z. Li, *A Study on the World's Shale Gas Resources Today*, Sino-Global Energy, 2014.

[3] Y. Luo, H. Liu, Y. Zhao, and G. Wang, "Effects of gas generation on stress states during burial and implications for natural fracture development," *Journal of Natural Gas Science and Engineering*, vol. 30, pp. 295–304, 2016.

[4] R. Wang, Y. Gu, W. Ding et al., "Characteristics and dominant controlling factors of organic-rich marine shales with high thermal maturity: A case study of the lower cambrian niutitang formation in the cen'gong block, southern China," *Journal of Natural Gas Science and Engineering*, vol. 33, pp. 81–96, 2016.

[5] Z. Wu, Y. Zuo, S. Wang et al., "Numerical simulation and fractal analysis of mesoscopic scale failure in shale using digital images," *Journal of Petroleum Science and Engineering*, vol. 145, pp. 592–599, 2016.

[6] Z. Wu, Y. Zuo, S. Wang et al., "Numerical study of multi-period palaeotectonic stress fields in lower cambrian shale reservoirs and the prediction of fractures distribution: a case study of the niutitang formation in Feng'gang No. 3 block, South China," *Marine and Petroleum Geology*, vol. 80, pp. 369–381, 2017.

[7] R. Yang, S. He, J. Yi, and Q. Hu, "Nano-scale pore structure and fractal dimension of organic-rich Wufeng-Longmaxi shale from Jiaoshiba area, Sichuan Basin: Investigations using FE-SEM, gas adsorption and helium pycnometry," *Marine and Petroleum Geology*, vol. 70, pp. 27–45, 2016.

[8] L. J. Dong, W. W. Shu, X. B. Li, Z. L. Zhou, F. Q. Gong, and X. L. Liu, "Quantitative evaluation and case study of risk degree for underground goafs with multiple indexes considering uncertain factors in mines," *Geofluids*, vol. 2, pp. 1–15, 2017.

[9] L. Dong, D. Sun, X. Li, and K. Du, "Theoretical and experimental studies of localization methodology for AE and microseismic sources without pre-measured wave velocity in mines," *IEEE Access*, vol. 5, pp. 16818–16828, 2017.

[10] L. Dong, W. Shu, X. Li, G. Han, and W. Zou, "Three dimensional comprehensive analytical solutions for locating sources of sensor networks in unknown velocity mining system," *IEEE Access*, vol. 5, pp. 11337–11351, 2017.

[11] Y. Cho, O. G. Apaydin, and E. Ozkan, "Pressure-dependent natural-fracture permeability in shale and its effect on shale-gas well production," *SPE Reservoir Evaluation and Engineering*, vol. 16, no. 2, pp. 216–228, 2013.

[12] Y. Xue, L. Cheng, J. Mou, and W. Zhao, "A new fracture prediction method by combining genetic algorithm with neural network in low-permeability reservoirs," *Journal of Petroleum Science and Engineering*, vol. 121, pp. 159–166, 2014.

[13] P. A. Hsieh, J. V. Tracy, C. E. Neuzil, J. D. Bredehoeft, and S. E. Silliman, "A transient laboratory method for determining the hydraulic properties of 'tight' rocks—I. Theory," *International Journal of Rock Mechanics and Mining Science and Geomechanics Abstracts*, vol. 18, pp. 245–252, 1981.

[14] C. E. Neuzil, C. Cooley, S. E. Silliman, J. D. Bredehoeft, and P. A. Hsieh, "A transient laboratory method for determining the hydraulic properties of 'tight' rocks-II. Application," *International Journal of Rock Mechanics and Mining Sciences and Geomechanics Abstracts*, vol. 18, no. 3, pp. 253–258, 1981.

[15] C. Hartman-Stroup, "The effect of organic matter type and organic carbon content on Rock-Eval hydrogen index in oil shales and source rocks," *Organic Geochemistry*, vol. 11, no. 5, pp. 351–369, 1987.

[16] S. C. Jones, "A technique for faster pulse-decay permeability measurements in tight rocks," *SPE Formation Evaluation*, vol. 12, no. 1, pp. 19–24, 1997.

[17] M. Josh, L. Esteban, C. Delle Piane, J. Sarout, D. N. Dewhurst, and M. B. Clennell, "Laboratory characterisation of shale properties," *Journal of Petroleum Science and Engineering*, vol. 88-89, pp. 107–124, 2012.

[18] A. Ghanizadeh, M. Gasparik, A. Amann-Hildenbrand, Y. Gensterblum, and B. M. Krooss, "Experimental study of fluid transport processes in the matrix system of the european organic-rich shales: I. scandinavian alum shale," *Marine and Petroleum Geology*, vol. 51, pp. 79–99, 2014.

[19] P. H. Nelson, "Pore-throat sizes in sandstones, tight sandstones, and shales," *AAPG Bulletin*, vol. 93, no. 3, pp. 329–340, 2009.

[20] M. A. Biot, "Theory of deformation of a porous viscoelastic anisotropic solid," *Journal of Applied Physics*, vol. 27, pp. 459–467, 1956.

[21] I. Fatt and D. H. Davis, "Reduction in Permeability With Overburden Pressure," *Society of Petroleum Engineers*, 1952.

[22] J. Geertsma, *The Effect of Fluid Pressure Decline on Volumetric Changes of Porous Rocks*, Petroleum Branch Fall Meeting, Los Angeles, Calif, USA, 1956.

[23] A. Lubinski, "The theory of elasticity for porous bodies displaying a strong pore structure," in *Proceedings of the 2nd US National Congress of Applied Mechanics*, pp. 247–256, 1954.

[24] J. G. Osorio, H. Chen, and L. W. Teufel, "Numerical simulation of coupled fluid-flow/geomechanical behavior of tight gas reservoirs with stress sensitive permeability," in *Proceedings of the Latin American and Caribbean Petroleum Engineering Conference*, Rio de Janeiro, Brazil, 1997.

[25] W. R. Jia, F. K. Li, and J. X. Xiao, "A study on some issues of development disposition of a low permeability oil field," *Petroleum Exploration and Development*, vol. 22, pp. 47–51, 1995.

[26] J.-J. Dong, J.-Y. Hsu, W.-J. Wu et al., "Stress-dependence of the permeability and porosity of sandstone and shale from TCDP

Hole-A," *International Journal of Rock Mechanics and Mining Sciences*, vol. 47, no. 7, pp. 1141–1157, 2010.

[27] G. R. L. Chalmers, D. J. K. Ross, and R. M. Bustin, "Geological controls on matrix permeability of devonian gas shales in the horn river and liard basins, northeastern British Columbia, Canada," *International Journal of Coal Geology*, vol. 103, pp. 120–131, 2012.

[28] O. Kwon, A. K. Kronenberg, A. F. Gangi, and B. Johnson, "Permeability of Wilcox shale and its effective pressure law," *Journal of Geophysical Research: Solid Earth*, vol. 106, no. 9, pp. 19339–19353, 2001.

[29] L. Reyes and S. O. Osisanya, "Empirical correlation of effective stress dependent shale rock properties," *Journal of Canadian Petroleum Technology*, vol. 41, no. 12, pp. 90–99, 2002.

[30] Z. Meng and G. Li, "Experimental research on the permeability of high-rank coal under a varying stress and its influencing factors," *Engineering Geology*, vol. 162, pp. 108–117, 2013.

[31] C. Li, "A theoretical formula of stress sensitivity index with compressibility of rock," *Lithologic Reservoirs*, vol. 19, pp. 95–98, 2007 (Chinese).

[32] M. Elgmati, *Shale Gas Rock Characterization and 3D Submicron Pore Network Reconstruction*, 2011.